

**Second and final report of EOARD-contract nr. F61708-97-W0237**

**Richard van de Sanden, Erwin Kessels, Daan Schram**  
**Department of Applied Physics**  
**Eindhoven University of Technology**  
**P.O.Box 513**  
**5600 MB Eindhoven**  
**The Netherlands**  
**Email: [m.c.m.v.d.sanden@phys.tue.nl](mailto:m.c.m.v.d.sanden@phys.tue.nl)**

DTIC QUALITY INSPECTED 4

19990903 202

AQF99-12-2193

REPORT DOCUMENTATION PAGE			Form Approved OMB No. 0704-0188	
Public reporting burden for this collection of information is estimated to average 1 hour per response, including the time for reviewing instructions, searching existing data sources, gathering and maintaining the data needed, and completing and reviewing the collection of information. Send comments regarding this burden estimate or any other aspect of this collection of information, including suggestions for reducing this burden to Washington Headquarters Services, Directorate for Information Operations and Reports, 1215 Jefferson Davis Highway, Suite 1204, Arlington, VA 22202-4302, and to the Office of Management and Budget, Paperwork Reduction Project (0704-0188), Washington, DC 20503.				
1. AGENCY USE ONLY (Leave blank)		2. REPORT DATE  1999		3. REPORT TYPE AND DATES COVERED  Final Report
4. TITLE AND SUBTITLE  Fast Deposition of Silicon Nitride and Aluminum Nitride on Nickel Titanium Substrates Using an Expanding Thermal Arc			5. FUNDING NUMBERS  F6170897W0237	
6. AUTHOR(S)  Dr. Richard van de Sanden				
7. PERFORMING ORGANIZATION NAME(S) AND ADDRESS(ES)  Eindhoven University of Technology PO Box 513 Eindhoven 5600 MB Netherlands			8. PERFORMING ORGANIZATION REPORT NUMBER  N/A	
9. SPONSORING/MONITORING AGENCY NAME(S) AND ADDRESS(ES)  EOARD PSC 802 BOX 14 FPO 09499-0200			10. SPONSORING/MONITORING AGENCY REPORT NUMBER  SPC 97-4082	
11. SUPPLEMENTARY NOTES				
12a. DISTRIBUTION/AVAILABILITY STATEMENT  Approved for public release; distribution is unlimited.			12b. DISTRIBUTION CODE  A	
13. ABSTRACT (Maximum 200 words)  This report results from a contract tasking Eindhoven University of Technology as follows: The contractor will investigate the feasibility of depositing SiNx or AlNx on substrates such as Ti or NiTi alloys. He will deliver samples of deposition. Also, he will transfer technology to USAF scientists at Wright Lab in Dayton Ohio....				
14. SUBJECT TERMS  EOARD, Plasma Sources, Applied Physics, Plasma Deposition and Etching			15. NUMBER OF PAGES  14	
			16. PRICE CODE N/A	
17. SECURITY CLASSIFICATION OF REPORT  UNCLASSIFIED	18. SECURITY CLASSIFICATION OF THIS PAGE  UNCLASSIFIED	19. SECURITY CLASSIFICATION OF ABSTRACT  UNCLASSIFIED	20. LIMITATION OF ABSTRACT  UL	

## **Project goals:**

This project deals with the development of a process to deposit silicon nitride and aluminum nitride on tantalum substrate using an expanding thermal plasma (ETP) source. This source enables the fast deposition of thick films in the range of 2 to 10  $\mu\text{m}$ . The project will make use of the infrastructure at the Eindhoven University of Technology and will be undertaken in close cooperation with Dr. B. Ganguly of Wright-Patterson Airforce Base (WPAFB) research labs.

## **Implementation**

In the first part of the project (see first report) the feasibility of deposition of  $\text{AlN}_x$  and  $\text{SiN}_x$  is investigated by means of a literature study. Especially the deposition of  $\text{AlN}_x$  poses problems and a possible route was suggested. However, the deposition of  $\text{SiN}_x$  was a relatively big success and in discussion with Dr. B. Ganguly during the Gordon Conference in Tilton it was decided to focus on  $\text{SiN}_x$  deposition. Relatively thick films of up to 2  $\mu\text{m}$  could be deposited with good adhesion on multi-crystalline silicon.

## **Deposition of silicon nitride on multi-crystalline silicon**

Two strategies to deposit  $\text{SiN}_x$  were utilized. The first way is the deposition by means of an expanding  $\text{Ar-N}_2(-\text{H}_2)$  plasma in which  $\text{SiH}_4$  is injected downstream. The second method involves the introduction of both  $\text{SiH}_4$  and  $\text{NH}_3$  in an expanding  $\text{Ar}(-\text{H}_2)$  plasma. The growth is monitored in situ by means of HeNe ellipsometry and ex situ by means of Fourier Transform Infrared Absorption Spectroscopy (FTIR) and Elastic Recoil Detection analysis (ERD).

## **Experiment**

A schematic illustration of the ETP setup is given in Figure 1. The plasma source is a dc operated cascaded arc in which non-depositing plasmas are created at subatmospheric pressure (about 400 mbar). For silicon nitride the plasma created in this source is an  $\text{Ar-N}_2(-\text{H}_2)$  plasma. The gas flows, given in standard cubic centimeter per second (sccs), and other discharge parameters are listed in Table 1. The pressure in the reactor chamber is kept at about 0.2 mbar and due to the pressure drop the plasma expands supersonically from the source into the reactor chamber. A stationary shock occurs at 4-6 cm from the arc exit after which the velocity is subsonic (typically 1000 m/s). Just behind the stationary shock deposition precursor gases, like  $\text{SiH}_4$  in this case, can be injected into the plasma by means of an injection ring. The  $\text{SiH}_4$  is dissociated by the reactive species emanating from the plasma source and leading to deposition. For more details about the plasma source and the deposition setup, the reader is referred to ref. [KES98b].

Substrate holders, on which three substrates of  $2.5 \times 2.5 \text{ cm}^2$  can be mounted, are positioned on a yoke 38 cm from the arc exit by means of a magnetic movable arm from

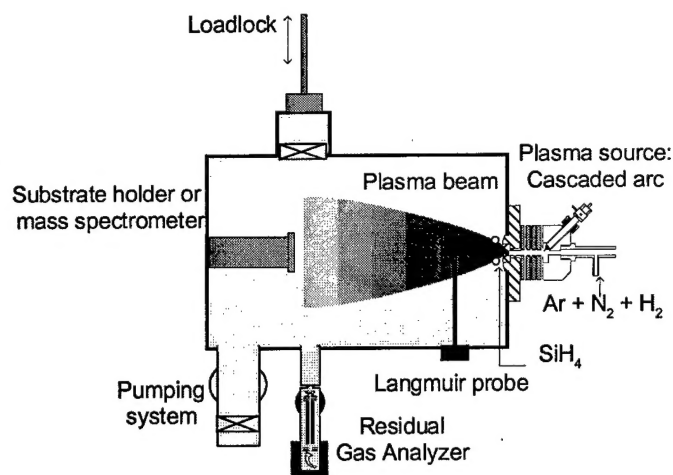


**Figure 1:** Expanding Thermal Plasma setup with gas injection for high growth rate silicon nitride deposition. The figure is not on scale.

a load lock system without venting the reactor. The yoke can be heated up to 500 °C. The thermal contact between yoke and holder and holder and substrate is optimized by a helium backflow leading to a temperature difference of at maximum 15 °C between yoke and substrates, even when the plasma is gated on [GIE96,SAN97].

Films of about 300 nm thickness deposited on p-type crystalline silicon substrates (500  $\mu\text{m}$ , 10-20  $\Omega\text{cm}$ ) are analyzed by ellipsometry, FTIR absorption spectroscopy and elastic recoil detection (ERD). From ellipsometry the refractive index (at 2 eV) and film thickness are determined. Information on the hydrogen content and on its bonding configurations is obtained by FTIR absorption spectroscopy. Therefore the peak positions  $\omega_{\text{max}}$  and calibration constants  $K$  for the hydrogen stretching modes as determined from a detailed study for different  $\text{a-Si}_x\text{N}_y\text{H}_z$  alloys by Bustarret et al. [BUS88] are used:  $\text{HSi-N}_2\text{Si}$  and  $\text{H}_2\text{Si-NSi}$  at  $\omega_{\text{max}}=2140\text{ cm}^{-1}$  ( $K=1.1\times 10^{20}\text{ cm}^{-2}$ ),  $\text{H}_2\text{Si-N}_2$  at  $\omega_{\text{max}}=2175\text{ cm}^{-1}$  ( $K=4.0\times 10^{20}\text{ cm}^{-2}$ ),  $\text{HSi-N}_3$  at  $\omega_{\text{max}}=2220\text{ cm}^{-1}$  ( $K=2.0\times 10^{20}\text{ cm}^{-2}$ ),  $\text{NH}$  at  $\omega_{\text{max}}=3335\text{ cm}^{-1}$  ( $K=1.2\times 10^{20}\text{ cm}^{-2}$ ),  $\text{NH}_2$  at  $\omega_{\text{max}}=3445\text{ cm}^{-1}$  ( $K=5\times 10^{20}\text{ cm}^{-2}$ ). From elastic recoil detection, using a 54 MeV  $^{65}\text{Cu}^{8+}$  beam [BIK93] information on the N, Si and H atomic densities in the films is obtained.

Arc current	45 A
Ar-flow	55 sccs
N <sub>2</sub> -flow	8 sccs
H <sub>2</sub> -flow	0-5 sccs
SiH <sub>4</sub> -flow	1-15 sccs
Downstream pressure	0.16-0.21 mbar
Substrate temperature	200-500 °C

**Table 1:** Discharge parameters for silicon nitride deposition at high growth rates.

More information on the gas-phase reactions and the species contributing to film growth is obtained by applying several plasma diagnostics to the non-depositing Ar-N<sub>2</sub>(-H<sub>2</sub>) carrier plasma used for SiH<sub>4</sub> decomposition. By means of a combination of Langmuir probe measurements and ion mass spectrometry the electron temperature, ion densities, dominant ions and the ion fluence from the plasma source are examined by a procedure similar as given in ref. [KES98c,KES98b]. The Langmuir probe measurements, using a single probe, have been performed at two axial positions (8 cm from the arc exit and 2 cm in front of the substrate holder) for different radial positions. Ion mass spectrometry has been performed at the position of the substrates by replacing the substrate holder with a Hiden EPIC 300 mass spectrometer. This mass spectrometer has also been used to analyze the flux of atomic nitrogen and atomic hydrogen at the substrate under non-depositing conditions. This was done by appearance potential or threshold ionization mass spectrometry which means that the energy of the electrons in the ionizer of the mass spectrometer is scanned to discriminate between ionization of radical species and the dissociative ionization of the parent neutrals [KAE95].

For the depositing plasma with SiH<sub>4</sub> the net consumed SiH<sub>4</sub> and N<sub>2</sub> flow have been determined from residual gas analysis. This is done by a Balzers Prisma 200 RGA positioned at the side of the reactor chamber and by a procedure similar to the one given in ref. [SAN98]. Furthermore, ion measurements have been carried out on this plasma by mass spectrometry and Langmuir probe measurements.

## Results

### A. Source and downstream plasma properties

To get insight in the downstream gas-phase reactions and the film growth precursors knowledge about the type and quantity of reactive species emanating from the plasma source is of utmost importance. For this reason, the non-depositing Ar-N<sub>2</sub>(-H<sub>2</sub>)

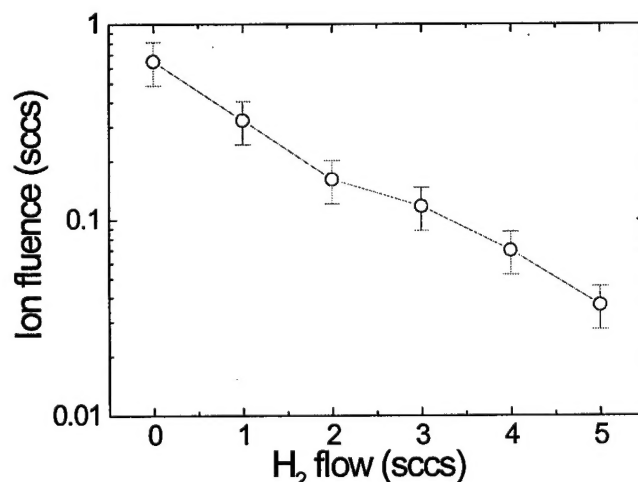


**Figure 2:** Ion fluence emanating from cascaded arc plasma source in standard cubic centimeters per second (sccs) as a function of H<sub>2</sub> admixture in the source. Other conditions: 55 sccs Ar, 10 sccs N<sub>2</sub> and 45 A arc current.

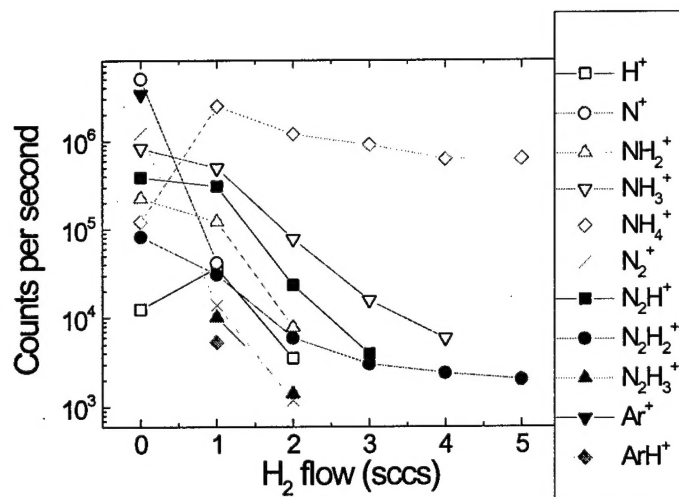


**Figure 3:** Type and abundance of ions emanating from the plasma source as obtained by ion mass spectrometry. Data not corrected for mass discrimination of mass spectrometer. The plasma conditions are given in Fig. 2.

plasma expanding from the cascaded arc plasma source has been subject of research. The electrons and ions have been studied by means of Langmuir probe measurements and ion mass spectrometry in a similar way as described in ref. [KES98b]. For the conditions given in Table 1 single Langmuir probe measurements at about 8 cm from the arc exit have revealed electron temperatures of 0.3-0.4 eV, rather independent of the H<sub>2</sub> flow admixed. This electron temperature is equal in magnitude to those found in other gas mixtures used in the ETP setup [SAN94,MEU95,BRU97,KES98b]. It makes precursor gas decomposition by means of electron impact negligible compared to dissociation by means of reactive heavy particles as ions and radicals. The ion fluence emanating from the arc has been determined from the probe measurements scanned in radial direction by means of the method described in ref. [SAN98,KES98b] and it is given in Fig. 2. The total ion fluence, given in standard cubic centimeter per second (1 sccs corresponds with  $2.5 \times 10^{19}$  particles per second), decreases as a function of H<sub>2</sub> admixture. The effective mass determined from the ratio of electron and ion saturation current [BRU97,KES98b] is in the range 14 to 20 AMU and indicates that ions containing a single N atom prevail. This is confirmed by ion mass spectrometry at 38 cm from the arc exit. Figure 3 shows the most abundant ions present in the plasma as a function of the H<sub>2</sub> flow. The data, which are not corrected for mass discrimination by the mass spectrometer [KES98b], show that for no H<sub>2</sub> flow the atomic nitrogen atom N<sup>+</sup> is dominant in accordance with a previous study [DAH94]. For non-zero H<sub>2</sub> flows, NH<sub>4</sub><sup>+</sup> is dominant. The latter ion is most probably created by reactions between N<sup>+</sup> ions emanating from the arc and H<sub>2</sub> in the downstream region of the plasma. Due to the high heavy particle temperature (~1 eV) inside the plasma source it is not very likely that molecular ions emanate from this

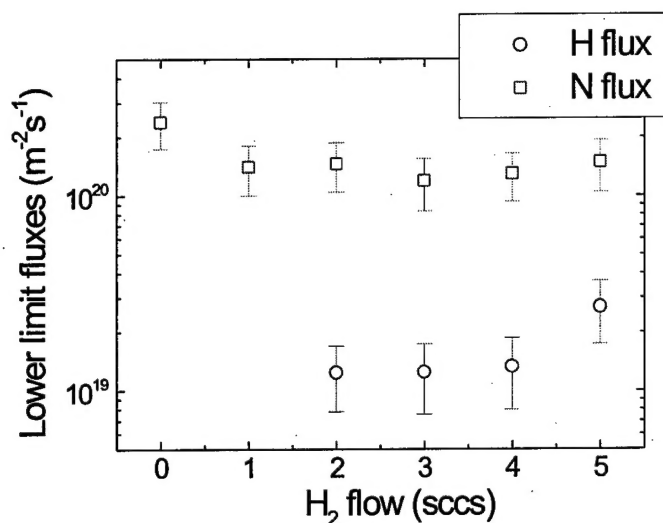


**Figure 4:** Lower limits of N and H radical fluxes on the substrate. For plasma conditions see Fig. 2.

source. It is unclear whether the formation of  $\text{NH}_4^+$  has already taken place before the ions reach the point where  $\text{SiH}_4$  is admixed to the plasma.

Another type of reactive species emanating from the plasma source are radicals like H and N. Studying the densities of these species requires advanced diagnostics as two-photon-absorption-laser-induced-fluorescence (TALIF) [MAZ99]. It is also possible to gain some insight in their presence and in their abundance by means of appearance potential or threshold ionization mass spectrometry [KAE95,SMI90]. For the present setup, it is only possible to investigate their fluxes at the position of the substrate holder, 38 cm from the arc exit. Another complication is the quantification of radical fluxes. In principle, the absolute fluxes can be obtained by relating the signal due to radicals to the signal due to parent molecules and accounting for difference in ionization cross sections [RAP65,MAR85,MCG68,CRO73]. The problems is however that radical species can get lost in their way from extraction orifice to the ionizer while stable molecules will not react and can easier build up a pressure inside the ionizer. The ratio of the intensities of the radicals and parent neutral does therefore not reflect the ratio of their fluxes at the substrate and only a lower limit for the thermal radical fluxes at the position of the substrate can be obtained with a good accuracy. In Fig. 4 the lower limit radical fluxes are given for H and N as function of the  $\text{H}_2$  flow admixed in the plasma source. The relatively high flux of atomic nitrogen is also interesting for application of the technique in nitration processes.

For the sake of completeness also the formation of  $\text{NH}_x$  ( $x=1,2$ ) radicals and of  $\text{NH}_3$  molecules in the Ar- $\text{N}_2$ - $\text{H}_2$  has been studied. No signal to the radicals mentioned could be observed by means of appearance potential mass spectrometry. The creation of  $\text{NH}_3$  on the other hand has been observed for the conditions in which  $\text{H}_2$  is admixed. By



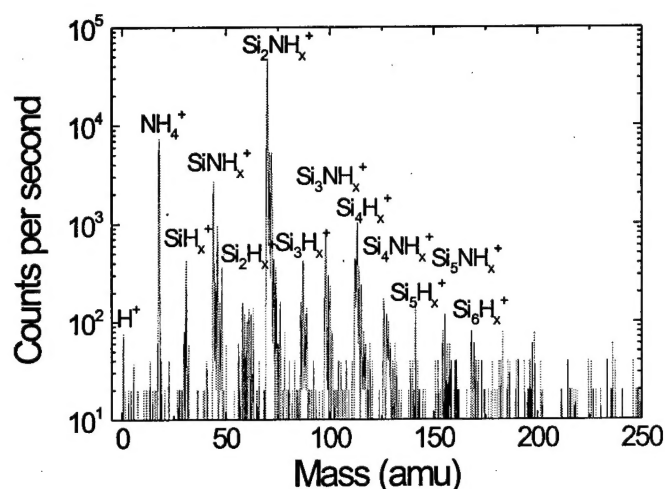


**Figure 5:** Ion mass spectrum measured at the position of the substrate for plasma condition in Fig. 2 and with a  $\text{H}_2$  and  $\text{SiH}_4$  flow of 5 sccs and 8 sccs respectively. Data not corrected for mass discrimination of mass spectrometer.

means of calibration with  $\text{NH}_3$  gas it turned out that the corresponding equivalent flow of generated  $\text{NH}_3$  in the  $\text{Ar-N}_2\text{-H}_2$  plasma is lower than 0.1 sccs for all conditions studied.

The study of the radicals created when  $\text{SiH}_4$  is added is even more complicated because a film is deposited and the gas extraction hole is eventually plugged. Up to now, this has prevented a detailed study on neutral species contributing to film growth. The detection of ionic species by mass spectrometry is on the other hand still possible due to their lower detection limit. A typical ion mass spectrum is shown in Figure 5. The spectrum, which is not corrected for mass discrimination [KES98b], shows ions up to about 250 amu. The noise is significant as the plugging of the mass spectrometers orifice limited the integration time feasible. The fact that the atomic mass of N is half the atomic mass of Si complicates the interpretation of the mass spectra. From similar observations of cationic silicon clusters in an expanding  $\text{Ar-H}_2\text{-SiH}_4$  plasma and from Ref. [KUS92] it is suggested that the ions observed are mainly  $\text{Si}_n\text{H}_m^+$  and  $\text{Si}_p\text{NH}_q^+$  ions. These ions are most probably created by subsequent ion-molecule reactions with  $\text{SiH}_4$  initiated by ions emanating from the plasma source [KES98b,KES98a]. The ions are also relatively hydrogen poor like in the  $\text{Ar-H}_2\text{-SiH}_4$  case. This has been attributed to the relatively high gas temperature [KES98b,KES98a,KES98c]. The fact that the  $\text{NH}_4^+$  signal remains relatively high upon  $\text{SiH}_4$  addition strongly suggests that it is not very reactive with  $\text{SiH}_4$  [KUS92]. This would indicate that the clustering reactions are mainly initiated by  $\text{N}^+$  ions reacting with  $\text{SiH}_4$  before all  $\text{N}^+$  is converted into  $\text{NH}_4^+$ .

An estimation of the contribution of the ions to the  $\text{SiH}_4$  growth flux is made from a combination of Langmuir probe measurements performed in front of the substrate holder [KES98b] and mass spectrometry. The contribution is estimated at 2-5 % assuming unity sticking probability of the Si containing ions. The accuracy is mainly limited by the fact that probe measurements are performed in a depositing plasma and by



SiH <sub>4</sub> flow (sccs)	H <sub>2</sub> flow (sccs)	Substrate temp. (°C)	Refractive index	Growth rate (nm/s)	[H] (10 <sup>22</sup> cm <sup>-3</sup> ) (at. %)		[Si] (10 <sup>22</sup> cm <sup>-3</sup> ) (at. %)		[N] (10 <sup>22</sup> cm <sup>-3</sup> ) (at. %)		density (g/cm <sup>3</sup> )	H bonding type
8	0	400	2.47	31.8	1.39	17.3	3.74	46.5	2.91	36.2	2.45	~90% SiH ~10% NH
8	1	400	2.40	25.3	1.19	16.3	3.43	46.9	2.70	36.9	2.25	~90% SiH ~10% NH
8	3	400	2.29	20.4	1.28	18.3	3.26	46.4	2.48	35.3	2.12	~100% SiH
8	5	400	2.33	19.4	1.23	17.4	3.42	48.4	2.41	34.2	2.19	~100% SiH
15	5	400	2.74	35.5	1.26	18.4	3.92	57.3	1.67	24.3	2.24	~100% SiH
4	5	400	1.99	13.2	1.20	16.4	2.83	38.6	3.30	45.0	2.12	~81% SiH ~19% NH
2	5	400	2.06	6.2	2.18	15.4	5.27	37.3	6.68	47.3	4.06	~100% NH <sub>x</sub> *
1	5	400	1.97	4.0	1.87	16.6	4.32	38.2	5.10	45.2	3.24	~100% NH <sub>x</sub> *
8	5	200	1.97	21.4	1.37	17.3	3.93	49.6	2.63	33.2	2.47	~80% SiH ~12% SiH <sub>2</sub> ~8% NH
8	5	300	2.21	20.4	1.68	20.9	3.88	48.2	2.49	30.9	2.42	~67% SiH ~29% SiH <sub>2</sub> ~4% NH
8	5	500	2.35	19.1	0.90	12.6	3.58	49.9	2.69	37.5	2.32	~100% SiH

\* A quantification of the NH<sub>x</sub> (x=1,2) bondings has not been possible. See text.

**Table 2:** Refractive index, growth rate, film atomic concentrations of hydrogen, silicon and nitrogen, mass density and the hydrogen bonding configurations for the silicon nitride films studied.

the fact that estimation of the average number of Si atoms in the ions is complicated by the appearance of  $H^+$  and  $NH_4^+$  in the ion spectrum. Taking mass discrimination of the mass spectrometer into account [KES98b], the average number of Si atoms is estimated at 2.4 from Fig. 5.

## B. Structural film properties

In order to map and to optimize the film properties that can be obtained with the ETP technique, the structural film properties of films deposited under various conditions have been analyzed. In Table 2, the refractive index, growth rate, film atomic composition, mass density as well as the H bonding configuration of the films are given for different  $H_2$  flows in the arc,  $SiH_4$  flows injected downstream and substrate temperatures. The refractive index (at 2 eV) and growth rate have been obtained by ex situ ellipsometry. The growth rate is in very good agreement with the growth rate determined by FTIR transmission spectroscopy. From Table 2, it is clear that high growth rates, up to 35 nm/s, can be obtained by the ETP technique. It is also possible to tune the refractive index between 1.7 and 2.8 by choosing the appropriate conditions. The atomic concentrations of H, Si and N are given in both atomic density and atomic percentage and have been obtained by Elastic Recoil Detection analysis. These data have been used in the calculation of the mass density of the films. Insight in the H bonding configuration has been obtained by FTIR transmission spectroscopy by using the calibration constants as determined by Bustarret et al. [BUS88]. The agreement between the hydrogen concentration as determined by FTIR and ERD is within 30%, except for two cases where the samples contain a significant amount of  $NH_2$  (absorption at  $3445\text{ cm}^{-1}$ ). This suggests that the calibration constant for hydrogen bonded as  $NH_2$  in the study of Bustarret et al. [BUS88] is most probably too high for the ETP material. Furthermore, some weak absorption peaks observed for conditions with a low  $SiH_4$  flow could not be attributed to a certain H bonding configuration unambiguously. Other differences are possibly due to the experimental accuracy and the dependence of the calibration constants on the overall film properties, which most probably also explains the discrepancies in calibration constants reported in literature [LAN78,KAP83,BUS88].

Varying the  $H_2$  flow in the arc from 0 sccs to 5 sccs while keeping the  $SiH_4$  flow and substrate temperature fixed at 8 sccs and  $400^\circ\text{C}$  respectively, yields a slight decrease in refractive index and a 50% decrease in growth rate. For no  $H_2$  admixture, the atomic densities of Si, N and H are higher than for the conditions with  $H_2$  admixture. The N/Si ratio is in the range of 0.7-0.8 and decreases slightly with increasing  $H_2$  admixture. The films are all Si-rich but interesting is the fact that the films deposited at 0 and 1 sccs  $H_2$  contain a considerable amount of NH bonded hydrogen (about 10%). The data are in agreement with the experimentally observed fact that hydrogen is usually relatively more bonded to nitrogen at higher N/Si ratios [BUS88,ROB91,LIN92]. The fact that hydrogen in high passivation quality films is observed to be mainly bonded to Si [LAU98] suggests that admixture of  $H_2$  in the arc improves the silicon nitride quality for surface passivation applications. Therefore, a  $H_2$  flow of 5 sccs in the arc is chosen throughout the following experiments.

The film properties are much more dependent on the  $SiH_4$  flow admixed in the downstream region. The refractive index and growth rate as a function of the  $SiH_4$  flow is given in Fig. 6. The growth rate and particularly the Si growth flux (product of growth

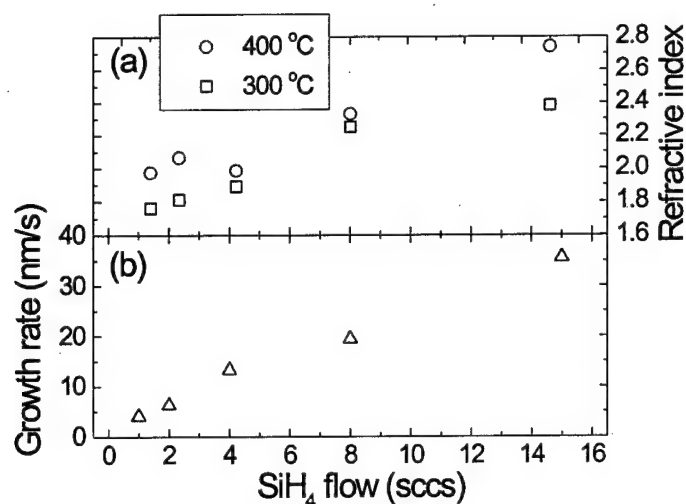


**Figure 6:** Refractive index (a) and growth rate (b) as a function of  $\text{SiH}_4$  flow for films deposited at substrate temperatures of 300 and 400 °C and with a  $\text{H}_2$  flow of 5 sccs.

rate and film silicon density) show a linear increase with  $\text{SiH}_4$  flow. The refractive index increases with increasing  $\text{SiH}_4$  flow and it is slightly higher for the 400 °C samples than for the 300 °C samples. The increase in refractive index corresponds with the decrease in the N/Si ratio as given in Fig. 7. This shows that the films can be changed from N-rich to Si-rich by increasing the  $\text{SiH}_4$  flow while keeping the  $\text{N}_2$  admixture in the arc constant. Moreover, the general trend that the film density increases with the N/Si ratio [GUR90, LAN78] is observed. The relative hydrogen content of the films is roughly 15-18% and shows no clear dependence on the  $\text{SiH}_4$  flow. The bonding configuration of the hydrogen changes however from a pure  $\text{NH}_x$  bonding type for low  $\text{SiH}_4$  flows to a pure SiH bonding type for higher  $\text{SiH}_4$  flows. This is in agreement with the transition from N-rich to Si-rich silicon nitride as also observed in other studies [BUS88, LIN92]. Silicon nitride films with a superior surface passivation quality, i.e. diminishing the electronic defects at the silicon surface, are in general Si-rich, whereas films with superior dielectric behavior are usually N-rich.

The influence of the substrate temperature is investigated in more detail for Si-rich samples deposited with 8 sccs  $\text{SiH}_4$ . In Table II, it can be seen that the growth rate slightly decreases with increasing substrate temperature whereas the refractive index increases. This is not simply due to a densification of the material as follows from the Si and N density as well as the mass density. The increase of refractive index is presumably due to a decreasing H density in the film (cf. Fig. 8). This figure shows that hydrogen bonded as  $\text{SiH}_x$  as well as hydrogen bonded as NH decrease for increasing temperatures. No significant amount of hydrogen bonded to nitrogen can be observed for temperatures above 300 °C. It can be concluded that substrate temperatures above 300 °C are necessary to avoid NH bonded hydrogen.

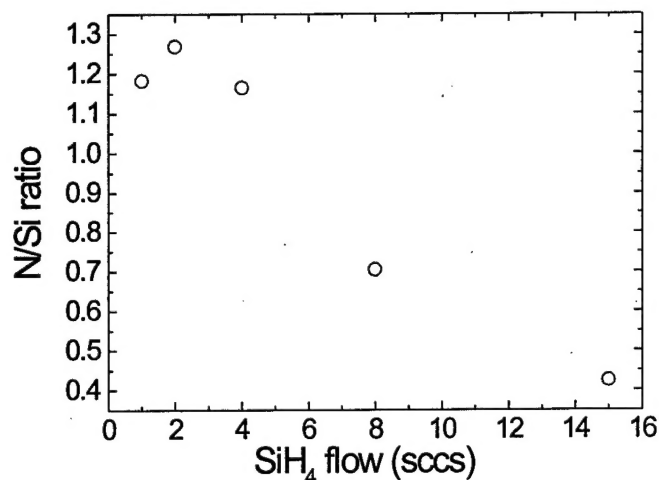


**Figure 7:** N/Si ratio determined by Elastic Recoil Detection analysis for films in Fig. 6 and a substrate temperature of 400 °C.

An interesting observation is the fact that the silicon growth flux as well as the nitrogen growth flux [END1] show a clear correlation with the depletion of the SiH<sub>4</sub> and N<sub>2</sub> flow respectively when the plasma is ignited. This suggests that the consumed SiH<sub>4</sub> and N<sub>2</sub> flow are mainly converted into the film and not in other stable gaseous products which are pumped away. Furthermore, monitoring the depletion of both gases yields a simple procedure to estimate roughly the N/Si ratio.

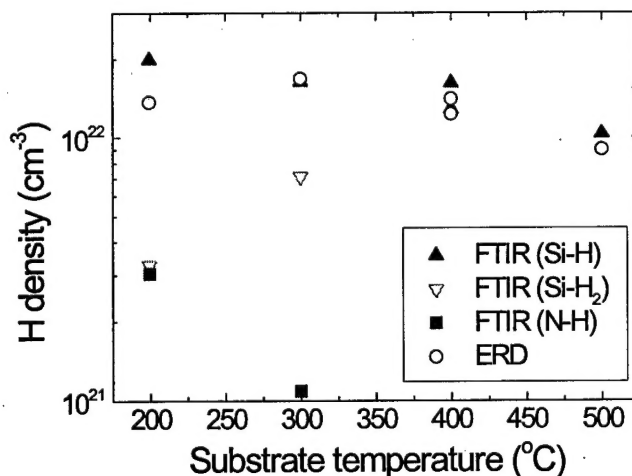


**Figure 8:** Atomic hydrogen density as determined from Elastic Recoil Detection analysis ([H]) and from FTIR absorption spectroscopy ([SiH], [NH]) for different substrate temperatures. The H<sub>2</sub> and SiH<sub>4</sub> flow are 5 and 8 sccs respectively.

## Discussion

In section A of the results, the reactive species emanating from the cascaded arc plasma source have been studied as a function of the  $H_2$  flow admixed in this source. From this, more insight in the reactions occurring in the plasma and finally leading to film growth can be gained. It has been shown that the role of electrons in the dissociation of  $SiH_4$  can be neglected due to the low electron temperature. Furthermore, the electron and ion fluence emanating from the source decreases drastically when a considerable amount of  $H_2$  is admixed. The depletion of  $SiH_4$  (for a  $SiH_4$  flow of 8 sccs) decreases from 85 to 60% when 5 sccs  $H_2$  is added and the depletion is well correlated with the Si growth flux. This decrease can be contributed to the decrease in ion fluence and N flux when  $H_2$  is admixed (cf. Fig. 4). However, the  $SiH_4$  consumption decreases much less than expected from the decrease of these fluxes. This implies that a considerable amount of  $SiH_4$  is dissociated by H emanating from the arc for non-zero  $H_2$  flows. Another explanation, a dependence of the reactivity of ions with  $SiH_4$  on the type of ions is less likely to cause the difference. Dominantly  $N^+$  emanates from the plasma source even when  $H_2$  is admixed. The type of ion dominantly reacting with  $SiH_4$  depends on the fact whether  $N^+$  has been able to react with  $SiH_4$  before reacting with  $H_2$  for non-zero  $H_2$  flows. The ion spectra for the non-depositing plasma (cf. Fig. 3) showed that  $N^+$  has mainly reacted to  $NH_4^+$  once it reaches the mass spectrometer, but it does not give any information on the case that  $SiH_4$  is admixed. Another point of interest is the fact that the  $SiH_4$  consumption during silicon nitride deposition exceeds the  $SiH_4$  consumption during a-Si:H deposition (12% for equal plasma conditions except for the  $N_2$  flow (= 0 sccs) [KES99]). This can be explained by an increased H flux from the arc when  $N_2$  is admixed. The latter was evidenced by appearance potential mass spectrometry. It cannot be explained by the ion-silane reactions as the ion fluence from the arc is lower in case of silicon nitride deposition [KES98b,SAN98]. Furthermore, the deposition is almost fully governed by radicals as there is only a very small contribution of  $Si_pN_qH_r^+$  ions to the silicon growth flux. The radical chemistry depends also on the reactions of N with  $SiH_4$ , which is relatively unknown. Hydrogen abstraction of  $SiH_4$  by N is endothermic by approximately 0.5 eV, about equal to the endothermicity for hydrogen abstraction of  $SiH_4$  by H. The reaction of N with  $SiH_4$  is not expected to be very significant [SMI90,KUS92]. If the latter is true, the silicon nitride deposition with the ETP technique can also be explained by deposition of an a-Si:H reaction layer which is nitrated by N radicals as proposed by Smith [SMI90] and corroborated by others [KUS92,HAN98].

It has been shown that films with a wide variety of N/Si ratios and consequently refractive indexes can be obtained by the ETP technique. This can be achieved by independently changing the plasma conditions, which is an advantage of remote deposition techniques over direct deposition techniques. The fact that a mixture of  $N_2$  and  $SiH_4$  can be used, in absence of ion bombardment (due to the low electron temperature) and at deposition rates which are 10 to 100 times higher compared to other techniques makes the ETP material for example interesting for the application as anti-reflection coating on crystalline silicon solar cells. Moreover, a relative high H flux during deposition and an H content of the material between 15 and 20% will lead most probably to an improved passivation of bulk defects and/or grain boundaries in multi-crystalline solar cells.

## Conclusions

Silicon nitride deposition by an expanding thermal plasma using  $N_2$  and  $SiH_4$  has been investigated by studying the plasma chemistry and the resulting film properties. The technique enables silicon nitride deposition at growth rates of 20 nm/s and tuning of the film atomic composition (N/Si ratio between 0.4 - 1.3) and refractive index (1.8-2.8) by changing plasma conditions independently. The application of high growth rate, remote plasma deposited silicon nitride as e.g. anti-reflection coating and passivation of bulk defects is promising for the fabrication of cost effective multi-crystalline solar cells.

## Acknowledgments

The authors greatly acknowledge R. ter Riet, J.C.M. Smits, A.H.M. Smets and B.A. Korevaar for their help during the experiments. J.D. Moschner and W.A. Bik are thanked for the ellipsometry and the ERD measurements respectively. M.J.F. van de Sande, H.M.M. de Jong, and A.B.M. Hüsken are thanked for their skilful technical assistance.

## References

- [BIK93] W.M. Arnold Bik, F.H.P.M. Habraken, Rep. Prog. Phys. **56**, 859 (1993).
- [BRU97] G.J.H. Brussaard, M.C.M. van de Sanden, and D.C. Schram, Phys. Plasmas **4**, 3077 (1997).
- [BUS88] E. Bustarret, M. Bensouda, M.C. Habrard, J.C. Bruyère, S. Poulin and S.C.
- [CRO73] A. Crowe and J.W. McConkey, J. Phys. B **6**, 2088 (1973).
- [DAH94] R.P. Dahiya, M.J. de Graaf, R.J. Severens, M.C.M. van de Sanden, and D.C. Schram, Phys. Plasmas **1**, 2086 (1994).
- [GIE96] J.W.A.M. Gielen, W.M.M. Kessels, M.C.M. van de Sanden, D.C. Schram, J. Appl. Phys. **82**, 2643 (1997).
- [GUR90] M.M. Guraya, H. Ascolani, G. Zampieri, J.I. Cisneros, J.H. Dias da Silva, and M.P. Cantão, Phys. Rev. B **42**, 5677 (1990).
- [HAN98] B.F. Hanyaloglu and E.S. Aydil, J. Vac. Sci. Technol. A **16**, 2794 (1998).
- [KAE95] P. Kae-Nune, J. Perrin, J. Guillon and J. Jolly, Plasma Sources Sci. Technol. **4**, 250 (1995).
- [KAP83] V.J. Kapoor, R.S. Bailey, J. Vac. Sci. Technol. A **1**, 600 (1983).
- [KES98a] W.M.M. Kessels, R.J. Severens, M.C.M. van de Sanden, D.C. Schram, J. Non-Cryst. Solids **227-230**, 133 (1998).
- [KES98b] W.M.M. Kessels, C.M. Leewis, M.C.M. van de Sanden, D.C. Schram, submitted for publication.
- [KES98c] W.M.M. Kessels, C.M. Leewis, A. Leroux, M.C.M. van de Sanden, D.C. Schram, to appear in J. Vac. Sci. Technol. A **17**, Jul/Aug (1999).
- [KES99] W.M.M. Kessels, A.H.M. Smets, B.A. Korevaar, G.J. Adriaenssens, M.C.M. van de Sanden, and D.C. Schram, accepted for publication in Mat. Res. Soc. Symp. Proc. **557** (1999).
- [KUS92] M.J. Kushner, J. Appl. Phys. **71**, 4173 (1992).
- [LAU98] T. Lauinger, J. Moschner, A.G. Aberle, R. Hezel, J. Vac. Sci. Technol. A **16**, 530 (1998).

- [LAN78] W.A. Langford and M.J. Rand, J. Appl. Phys. **49**, 2473 (1978).
- [LIN92] K.-C. Lin and S.-C. Lee, J. Appl. Phys. **72**, 5474 (1992).
- [MAR85] T.D. Märk and G.H. Dunn, Electron Impact Ionization, ed. by T.D. Märk and G.H. Dunn, Springer-Verlag, Wien (1985).
- [MAZZ99] S. Mazouffre, M.G.H. Boogaarts, M.C.M. van de Sanden, J.A.M. van der Mullen, and D.C. Schram, to be published.
- [McG68] J.W. McGowan and E.M. Clarke, Phys. Rev. **167**, 43 (1968).
- [MEU95] R.F.G. Meulenbroeks, R.A.H. Engeln, M.N.A. Beurskens, R.M.J. Paffen, M.C.M. van de Sanden, J.A.M. van der Mullen, and D.C. Schram, Plasma Source Sci. Technol. **4**, 74 (1995).
- [ROB91] J. Robertson, Phil. Mag. B **63**, 47 (1991). [SAN97] M.C.M. van de Sanden, R.J. Severens, W.M.M. Kessels, L.J. van IJzendoorn and D.C. Schram, Mat. Res. Soc. Symp. Vol. **467** (1997), 621.
- [SAN98] M.C.M. van de Sanden, R.J. Severens, W.M.M. Kessels, R.F.G. Meulenbroeks, and D.C. Schram, J. Appl. Phys. **84**, 2426 (1998).
- [SAN94] M.C.M. van de Sanden, R. van den Bercken and D.C. Schram, Plasma Sources. Sci. Technol. **3**, 511 (1994).
- [SMI90] D.L. Smith, J. Vac. Sci. Technol. B **8**, 551 (1990)
- [STE94] A.W. Stephens, A.G. Aberle, and M.A. Green, J. Appl. Phys. **75**, 1611 (1994).
- [END1] Growth flux is defined as the product of film growth rate and atomic concentration in the film.